KOH CONCENTRATION EFFECT ON THE CYCLE LIFE OF NICKEL-HYDROGEN CELLS. IV. RESULTS OF FAILURE ANALYSES

H.S. Lim and S.A. Verzwyvelt
Hughes Aircraft Company
Los Angeles, California 90009

KOH concentration effects on cycle life of a Ni/H_2 cell have been studied by carrying out a cycle life test of ten Ni/H_2 boiler plate cells which contain electrolytes of various KOH concentrations. Failure analyses of these cells were carried out after completion of the life test which accumulated up to 40,000 cycles at an 80% depth of discharge over a period of 3.7 years. These failure analyses included studies on changes of electrical characteristics of test cells and component analyses after disassembly of the cell. The component analyses included visual inspections, dimensional changes, capacity measurements of nickel electrodes, scanning electron microscopy, BET surface area measurements, and chemical analyses. Results have indicated that failure mode and change in the nickel electrode varied as the concentration was varied, especially, when the concentration was changed from 31% or higher to 26% or lower.

INTRODUCTION

Long cycle life has been demanded for a Ni/H_2 cell at deep depth of discharge cycles used in spacecraft applications, especially for a low earth orbit (LEO). We have reported earlier that cycle life of Ni/H_2 cells was improved tremendously by using lower KOH concentrations in electrolyte than conventional 31% KOH[1]. The cycle life has been improved as much as nine times by simply changing the concentration to 26% (by weight) from a conventional value of 31%. A cycle life test has been completed for ten Ni/H_2 cells containing electrolytes of various KOH concentrations ranging from 21 to 36%. In the present paper, we report failure analysis results of these cells which include studies on changes of cell performance and cell components after cell disassembly. We have also studied electrochemical behavior of the cycled nickel electrodes. This result will be reported later.

EFFECTS OF KOH CONCENTRATION ON CYCLE LIFE

A cycle life test was carried out in a 45-min LEO regime at 80% depth of discharge on ten Ni/H_2 boiler plate cells containing electrolytes of 21 to 36% KOH. Test period covered 3 years and 8 months and accumulated up to 39,573 life cycles. Details of the cycle regime have been reported earlier.[1] Life test results are summarized in Table 1. All cells of relatively short cycle life (BP3 to 6) failed by low end-of-discharge voltage (EODV), while all cells of long cycle life (BP1, 2, 9, and 10) failed the cycling test due to a "soft" short formation which was indicated by rapid self-discharge. Fully charged cells discharged completely in 30 to 35 h. The effect of the concentration on cycle life is shown in Figure 1 and 2. The cycle life to 0.9 V of EODV peaked at 26% KOH showing tremendous improvement (about nine times) over the conventional electrolyte of 31% KOH, but the life decreased sharply when the concentration was lowered further below 26%. If the voltage criteria for failure was lowered to 0.5 V, however, KOH concentrations as low as 21% also gave the extreme long life (Fig. 2). This rather drastic change in cycle life by a small change in the voltage criteria was due to development of a large capacity having a low discharge voltage (about 0.8 V) plateau which is often refered as "the second plateau."[1]

TABLE 1. LIFE TEST RESULTS OF NI/H_2 CELLS AT 80% DEPTH-OF-DISCHARGE

CELL NO.	[KOH] %	NO.CYCLE TO 0.9 V	NO.CYCLE TO 0.5 V	TOTAL NO.CYCLES	FAILURE MODE
BP1	21	5,047	>38,191	38,191	SOFT SHORT
BP2	26	39,230	>39,573	39,573	SOFT SHORT
BP3	26	4,329	9,241	9,241	LOW EODV
BP4	31	2,979	3,275	3,286	LOW EODV
BP5	31	3,620	4,230	4,230	LOW EODV
BP6	36	1,268	1,845	1,845	LOW EODV
BP7*	21	1,037	6,508	9,402	LOW EODV
BP8	26	>30,549	>30,549	30,549	REMOVED
BP9	26	23,598	>24,594	24,594	SOFT SHORT
BP10	23.5	4,803	28,495	28,495	SOFT SHORT

* CYCLED AT 70% DEPTH-OF-DISCHARGE (DOD) FROM 1644 TO 4644 CYCLES AND AFTER 6508 CYCLES.

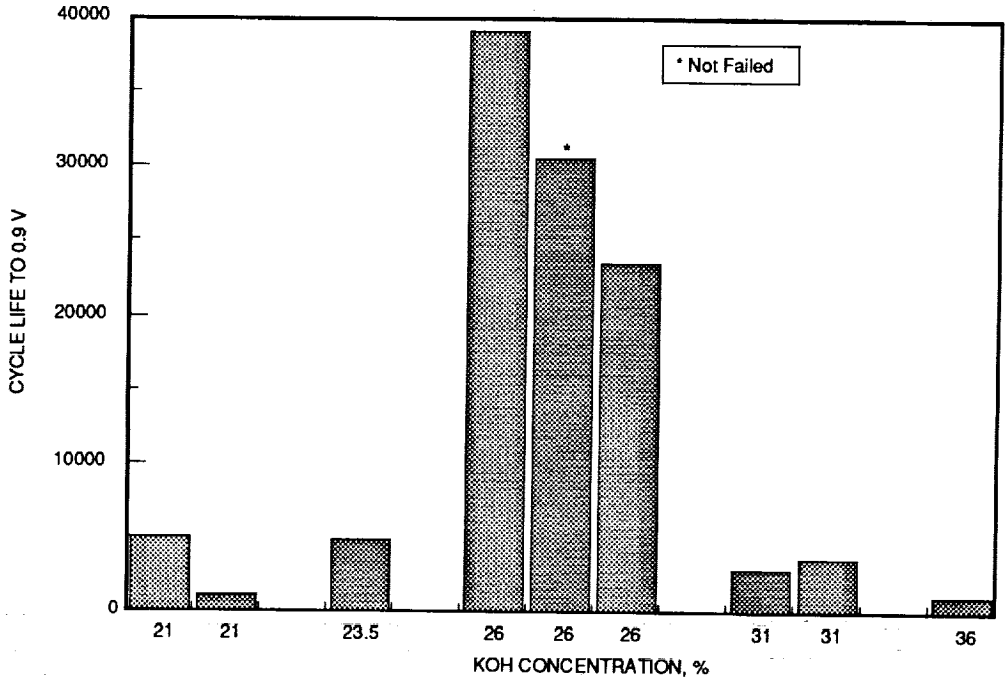

FIGURE 1. COMPARISON OF CYCLE LIFE TO 0.9 V OF Ni/H_2 CELLS WITH VARIOUS KOH CONCENTRATIONS IN THE ELECTROLYTE.

CHANGE OF CELL CHARACTERISTICS AFTER LIFE TEST

A series of duplicate to triplicate capacity measurements were carried out before and after the cycle life test using various charge and discharge rates in order to evaluate the rate effects on cell capacity. The charge rate effect was studied by measuring cell capacity at C/2 discharge rate to 1.0 V after charging them at C/10 rate for 16 h, C/2 rate for 160 min, C rate for 80 min, and 2C rate for 40 min, respectively. The discharge rate effect was studied by measuring cell capacity at various discharge rates (C/10, C/2, 1.0C, 1.37C, 2.0C, 2.74C, and 4.0C) to 1.0 V after charging them at C rate for 80 min. Internal resistance of cells was evaluated from mid-discharge voltages at various discharge rates.

Charge Rate Effects on Cell Capacity - Initial and end-of-life (EOL) capacity values are plotted against charge rates in Figure 3 and 4. The capacities of all cells improved as the charge rate increased from 0.1 to 0.5 C rate. This trend was more pronounced after the cycle test. Further increase in charge

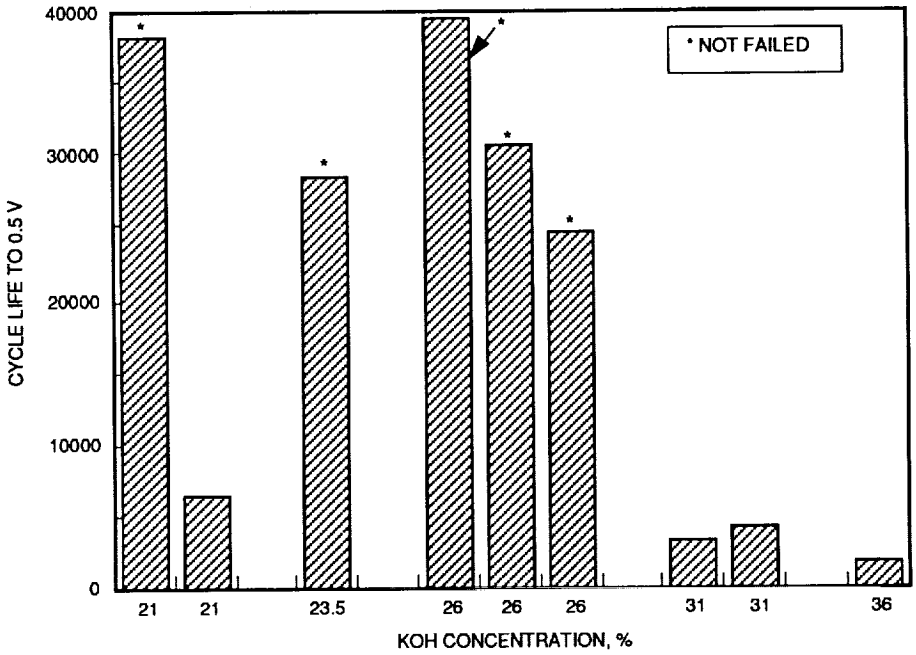

FIG. 2. COMPARISON OF CYCLE LIFE TO 0.5 V OF Ni/H_2 CELLS WITH VARIOUS KOH CONCENTRATIONS IN THE ELECTROLYTE.

rate over 0.5 C did not affect capacity of cells with high KOH concentrations (31 and 36%) while capacity of cells with low KOH concentrations improved slightly at 1 C rate. Capacities of all cells leveled off for the charge rates between 1 and 2 C. Although absolute values of the capacity decreased after life test with exception of BP8 and 10, general pattern of the charge rate dependence did not change with the cycle test.

Effects Of Discharge Rates On Capacity - Initial and EOL capacity values are plotted against discharge rates in Figure 5 and 6. Capacity of cells in general decreased slightly as discharge rate increased. This dependence of the capacity on discharge rate became more pronounced after the life test. We had also observed such dependence earlier with another group of 31% KOH cells.[2]

Cell Resistance - Plots of mid-discharge voltages (measured during the initial and EOL capacity tests) against the discharge current gave good straight lines as shown in Figure 7 for an illustration. The slopes of these lines represent the values of cell resistance. The cell resistances before and after the cycle life test are summarized in Table 2. Cell resistance did not appear to have changed significantly after the cycle life test except for BP1, BP3, and BP10. BP1 showed a significant reduction of the resistance. BP3 which had a defective current collector tab on one of the H_2 electrodes showed a significant increase. Overall, the change in the cell resistance with cycling appear to be too small to account either for the change of capacity dependence on discharge rate or to be the cause of cell failure.

COMPONENT ANALYSES AFTER CELL TEARDOWN

After the post-life-test capacity measurements, test cells were charged for 80 min at C rate and then discharged at C/2 rate to 0.5 V followed by shorting them with a 1.0-Ω resistance for a minimum of 24 h before disassembly of the cells for component study. This study included visual inspections during the

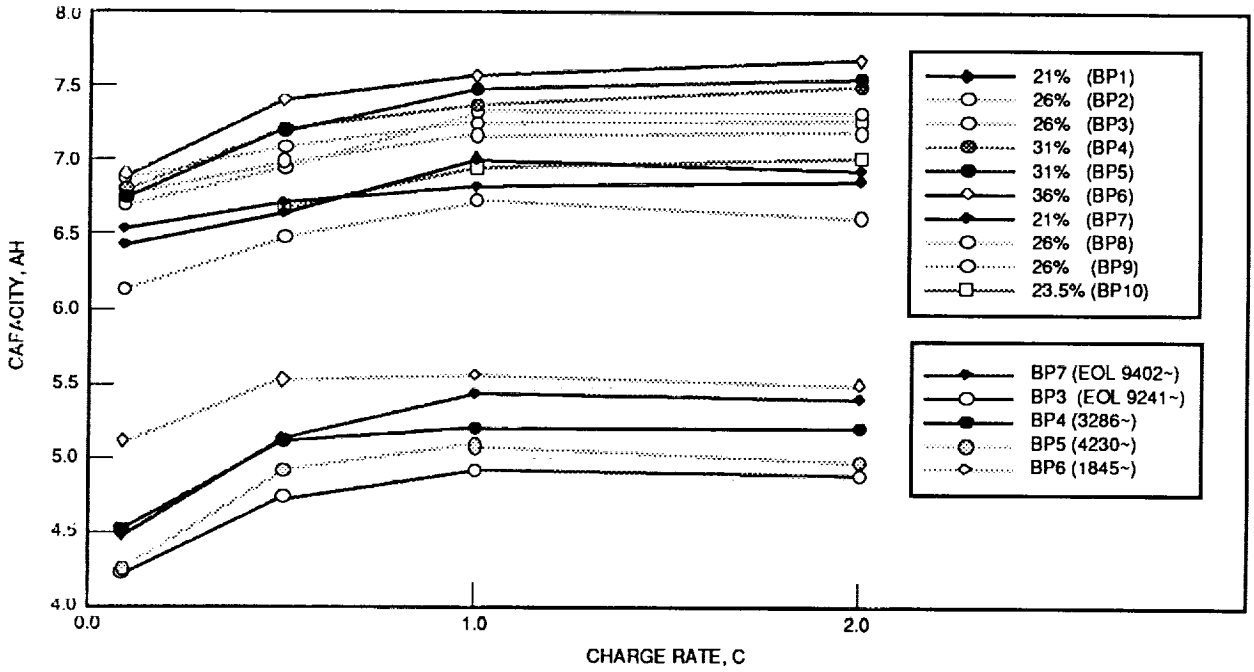

FIGURE 3. PLOTS OF INITIAL AND EOL CAPACITIES VS. CHARGE RATES. CAPACITY WAS MEASURED BY 0.5 C RATE DISCHARGE TO 1.0 V AFTER CHARGING AT VARIOUS RATES: 0.1 C RATE FOR 16 H, 0.5 C FOR 160 MIN., 1.0 C FOR 80 MIN., OR 2.0 C FOR 40 MIN.

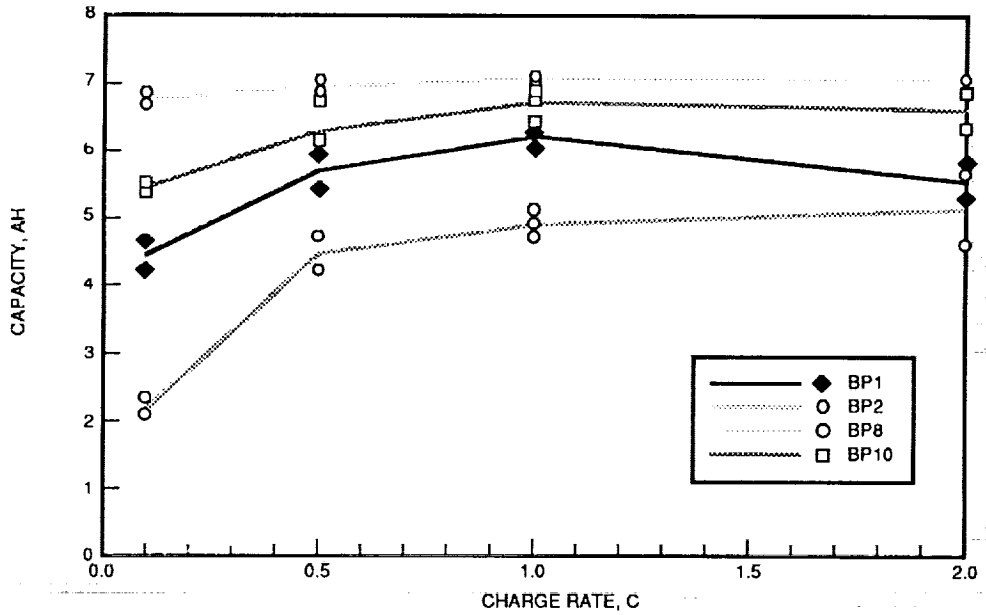

FIGURE 4. PLOTS OF EOL CAPACITIES VS CHARGE RATES. CAPACITY WAS MEASURED BY 0.5 C RATE DISCHARGE TO 1.0 V AFTER CHARGING AT VARIOUS RATES: 0.1 C RATE FOR 16 H, 0.5 C FOR 160 MIN., 1.0 C FOR 80 MIN., OR 2.0 C FOR 40 MIN.

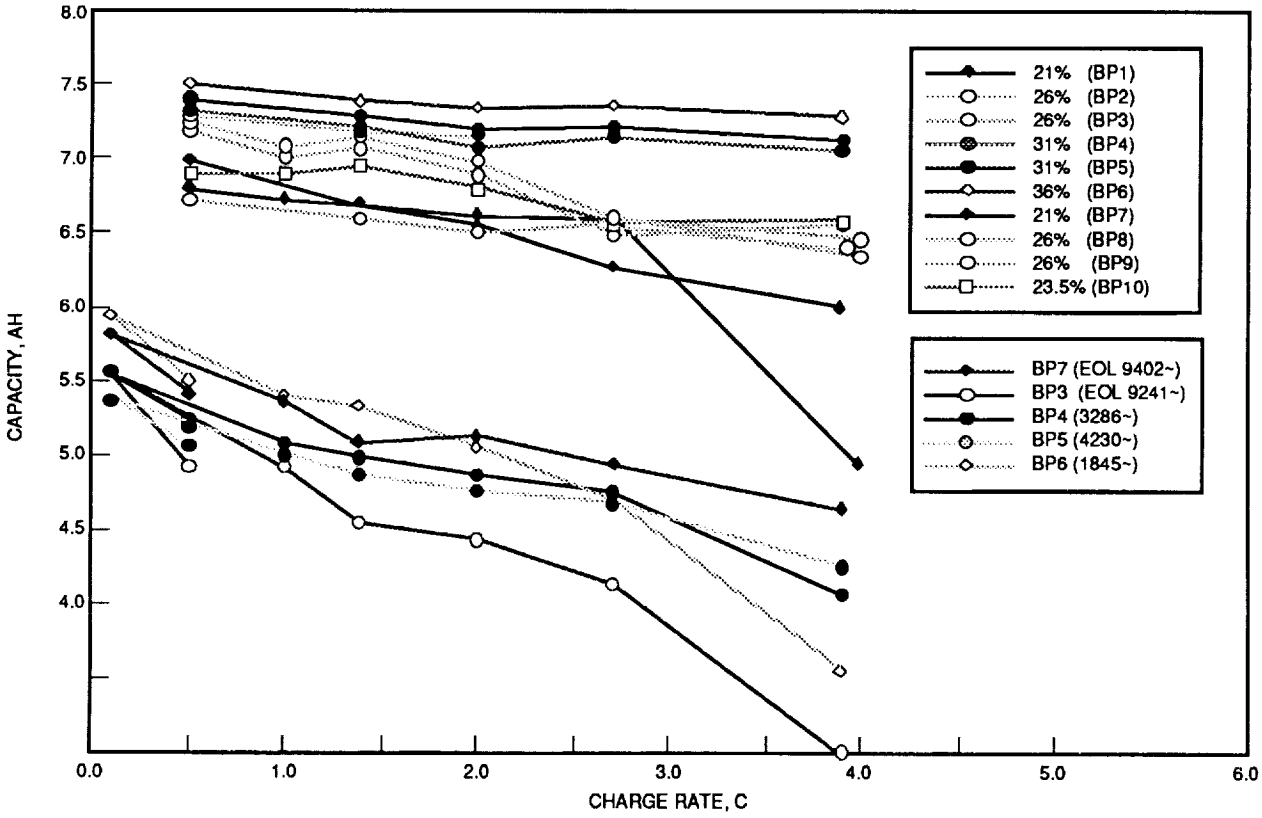

FIGURE 5. PLOTS OF INITIAL AND EOL CAPACITIES VS. CHARGE RATES. CAPACITY WAS MEASURED BY DISCHARGING CELLS AT VARIOUS RATES TO 1.0 V AFTER 1.0 C RATE CHARGE FOR 80 MIN.

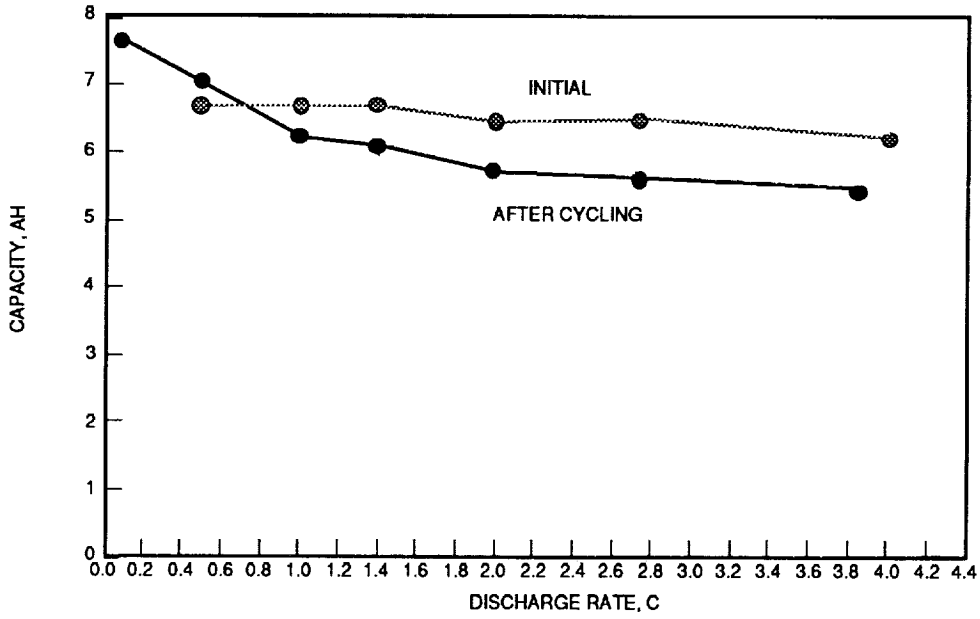

FIGURE 6. PLOTS OF INITIAL AND EOL CAPACITIES OF BP8 VS DISCHARGE RATES. CAPACITY WAS MEASURED BY DISCHARGING THE CELL AT VARIOUS RATES TO 1.0 V AFTER 1.0 C RATE CHARGE FOR 80 MIN.

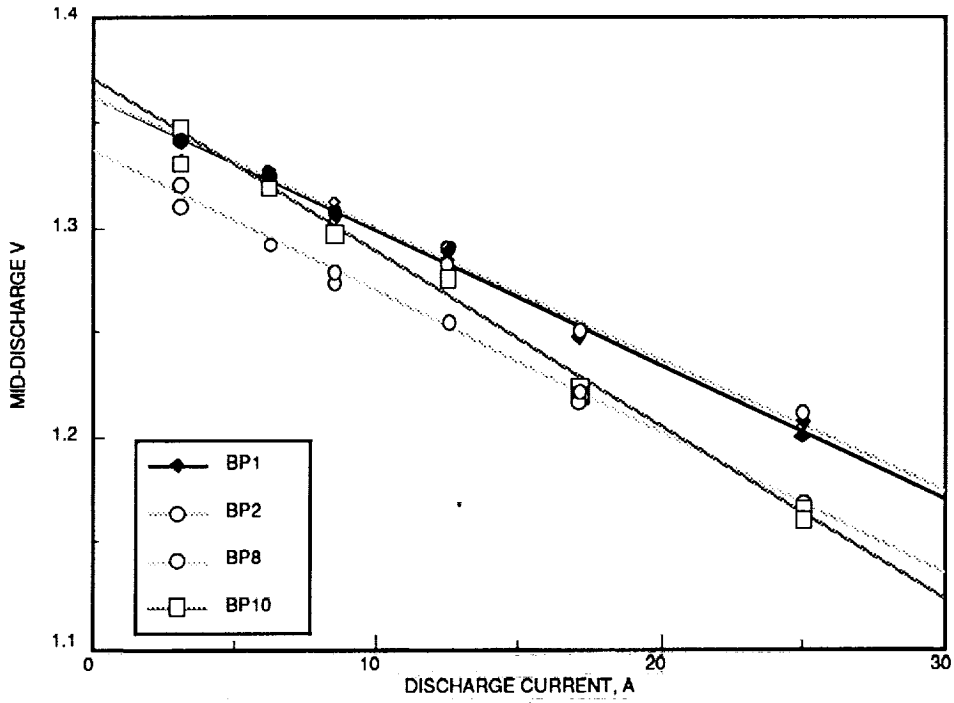

FIGURE 7. PLOTS OF MID-DISCHARGE VOLTAGES OF TEST CELLS VS DISCHARGE RATES FOR END-OF-LIFE PERFORMANCE TEST.

TABLE 2. CELL RESISTANCE (R) MEASURED FROM MID-DISCHARGE VOLTAGES.

CELL NO.	KOH %	NUMBER OF CYCLES	INITIAL R mΩ	EOL R mΩ	CHANGE mΩ	CELL P* PSIG
BP1	21.0	38,191	10.83	6.36	- 4.47	615
BP2	26.0	39,573	(5.89)	6.26	+ 0.37	705
BP3	26.0	9,241	7.53	9.69	+ 2.16	130
BP4	31.0	3,286	7.15	8.26	+ 1.11	150
BP5	31.0	4,230	7.09	6.96	- 0.13	225
BP6	36.0	1,845	7.61	8.49	+ 0.88	160
BP7	21.0	9,402	7.30	7.14	- 0.16	130
BP8	26.0	30,549	6.59	6.71	+ 0.12	0
BP10	23.5	28,495	6.57	8.24	+ 1.67	635

* PRESSURE PRIOR TO DISASSEMBLY.

disassembly, electrode thickness measurements (without washing and drying), scanning electron microscopy (SEM) of the cross-section of cell stacks, surface area measurements using BET technique, measurements of nickel electrode capacity and discharge voltages in flooded electrolyte cells, and chemical analyses of the nickel electrodes.

Visual Inspections - Conditions of cell stack and its components have been inspected carefully during disassembly of cycled cells. These inspections included wetness of components, degree of loose black nickel active material ("black powder") on cell components, penetration of the active material through the separator, adhesion of hydrogen electrode to gas screen, and integrity of nickel and hydrogen electrodes. Observations which appear to be important are summarized as follows:

- Wetness of the electrode and the degree of "black powder" formation increased noticeably as one approached the bottom of the stack (no.6 unit cell) from the top (no.1 unit cell). The observation on

wetness change indicated that gravitational effect on the electrolyte distribution is substantial even in this relatively short stack. The observation on "black powder" formation appears to indicate that a wetter unit cell might have been used more heavily than a drier unit cell.

- Electrodes from BP7 (21% KOH; 9402 cycles) showed noticeably less "black powder" on the adjacent separator and in gas screen than those from high KOH concentration cells which had lower number of cycles. The black powder in the gas screen was found only in the peripheral area of the stack with BP7 while it was found all over the screen with the other cells which were cycled less than BP7. However, the 21% KOH cell (BP1; 38,191 cycles) which were cycled much longer showed heavy black powdering. It appears that rate of black powder formation is reduced as KOH concentration decreased.

- Electrical lead (tab) of #5 H_2 electrode of BP3 was not firmly attached (defective weld) to the electrode while its paired nickel electrode and separator appeared new (almost without the black powder). This observation strongly indicates that the cause of the poor performance of this cell from the beginning was due to this poor electrical contact. The BP3 should be considered as an anomalous cell.

- All nickel electrodes from cells which had extremely long cycle life ($\geq$24,594 cycles) showed "mushy" appearance indicating that some active material has loosened and squeezed out of the sinter structure. This indication was confirmed by scanning electron microscopic (SEM) pictures as will be discussed later in this report.

- All cells which had extremely long cycle life ($\geq$24,594 cycles) showed the following: Outer edges of gas screen were welded to Teflon layer of the H_2 electrodes. Damage with partially lost electrode material were apparent on parts of peripheral area of electrode stacks. The outer coined nickel electrodes was badly eroded. These observations indicated that violent recombinations of O_2 with H_2 had occurred around peripheral area of electrode stacks during the cycling test period.

Pressure Changes - Gas pressure of test cells in the fully discharged state were measured just before their disassembly using a mechanical pressure gauge. This was done in order to determine the net pressure change during the cycle life test. Gas composition was analyzed using a gas chromatograph. Gases in all cells were pure hydrogen within experimental error. Results on pressure readings are shown in Table 2. Long cycled cells (BP1, 2, and 10) showed roughly 470 psi higher pressure than those of relatively short cycle life (BP4, 5, and 6). (BP8 might have leaked slowly.) Although the long term sealing reliability of presently used boiler plate cell cases was questionable as discussed earlier,[1b] the pressure increase in long cycled cells has be real. This pressure increase appears to be due to nickel corrosion from the sintered plaques probably according to equation (1):

$$Ni + 2H_2O \longrightarrow Ni(OH)_2 + H_2 \qquad (1)$$

Dimensional Changes of Stack Components - Thickness of nickel electrodes was measured by a micrometer at three different locations on each electrode before and after cycling. The thickness after cycling was measured both before and after rinsing out the electrolyte and drying. These two values agreed with each other within experimental error. The average values of these measurements for each electrode are tabulated in Table 3. Long cycled electrodes (BP2 and BP8) showed expansion values

up to 80% of the original thickness. These long cycled electrodes showed heavy extrusion of active material out of the electrode into voids of the gas screen. Typically imprints of gas screen are clearly visible when gas screen is separated from the electrode. The high value of expansion (up to 80%) was due to contribution of this extruded material.

Average expansion values of electrodes from individual cells are plotted against number of cycles in Figure 8. The expansion values appear to fall on a straight line eventhough the individual cells have different KOH concentrations. This observation appears to indicate that the expansion rate on long term cycling is rather insensitive to KOH concentration which is contrary to our earlier understanding.[3,4,5] The expansion itself does not appear to be the main cause of electrode or cell failure.

TABLE 3. NICKEL ELECTRODE EXPANSION AFTER CYCLE TEST IN NI/H_2 CELLS WITH VARIOUS KOH CONCENTRATIONS.

CELL (%KOH) (CYCLE NO)	ELECTRODE I.D.	THICKNESS AFTER CYCLING,* MM	THICKNESS BEFORE CYCLING, MM	EXPANSION* %
BP1 (21%) (31,191)	28-05(#1, TOP)	1.166	0.761	53.4
	28-04(#2)	1.141	0.758	50.5
	24-03(#5)	1.268	0.737	71.8
	24-01(#6, BOTTOM)	1.225	0.751	63.2
BP2 (26%) (39, 573)	20-01(#1)	1.310	0.732	79.0
	20-02(#2)	1.274	0.739	72.5
	19-05(#5)	1.341	0.737	81.8
	19-06(#6)	1.327	0.735	76.1
BP3 (26%) (9641)	25-01(#1)	0.930	0.768	21.1
	26-02	0.933	0.744	25.3
	35-03(AN)	0.762	0.750	1.6
	35-04(#6)	0.947	0.753	25.7
BP4 (31%) (3275)	25-09(#1)	0.837	0.727	15.1
	26-03	0.814	0.732	11.2
	26-09	0.819	0.755	8.5
	27-07 (#6)	0.778	0.744	4.6
BP5 (31%) (4230)	22-02 (#1)	0.809	0.738	9.6
	22-03	0.814	0.732	13.6
	22-09	0.785	0.721	8.9
	20-03 (#6)	0.758	0.755	0.4
BP6 (36%) (1845)	27-03(#1)	0.816	0.744	9.6
	27-05	0.777	0.720	7.8
	35-08	0.785	0.724	8.4
	35-09(#6)	0.771	0.723	6.7
BP7 (21%) (9402)	05-05(#1)	0.876	0.748	17.2
	05-06(#2)	0.916	0.746	22.7
	21-07(#3)	0.929	0.755	23.1
	21-08(#4)	0.949	0.755	25.6
BP8 (26%) (30,549)	21-05(#1)	1.225	0.728	68.2
	21-01(#2)	1.286	0.762	68.7
	03-06(#5)	1.297	0.727	78.4
	03-02(#6)	1.304	0.719	81.3
BP9(26%) (24,594)	03-03(#1)	1.217	0.736	65.4
	04-07(#2)	1.229	0.735	63.2
	04-07(#5)	1.233	0.741	66.4
	06-07(#6)	1.208	0.752	60.6
BP10 (23.5%) (28,495)	04-03(#1)	1.330	0.751	77.2
	16-05(#2)	1.281	0.736	74.1
	16-02(#5)	1.353	0.760	78.0
	16-09(#6)	1.285	0.746	72.1

* MEASURED VALUES INCLUDE EXTRUDED ACTIVE MATERIAL INTO VOIDS OF GAS SCREEN.

Thickness of stack components including separator and gas screen was also measured from SEM picture of cross-section of cell stack. The results are shown in Figure 9 as a function of the number of cycles. Dimension of unit cell was generally unchanged with cycling. Nickel electrode expansion was again roughly linear with the number of cycles. Separator and gas screen were compressed as the nickel electrode expanded.

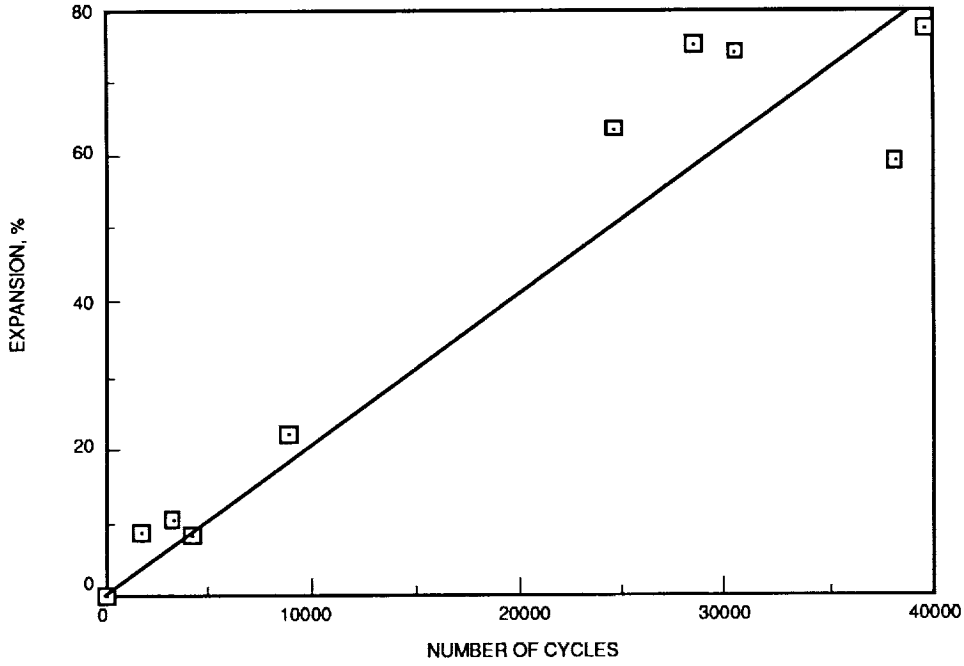

FIGURE 8. A PLOT OF NICKEL ELECTRODE EXPANSION VS. NUMBER OF CYCLES.

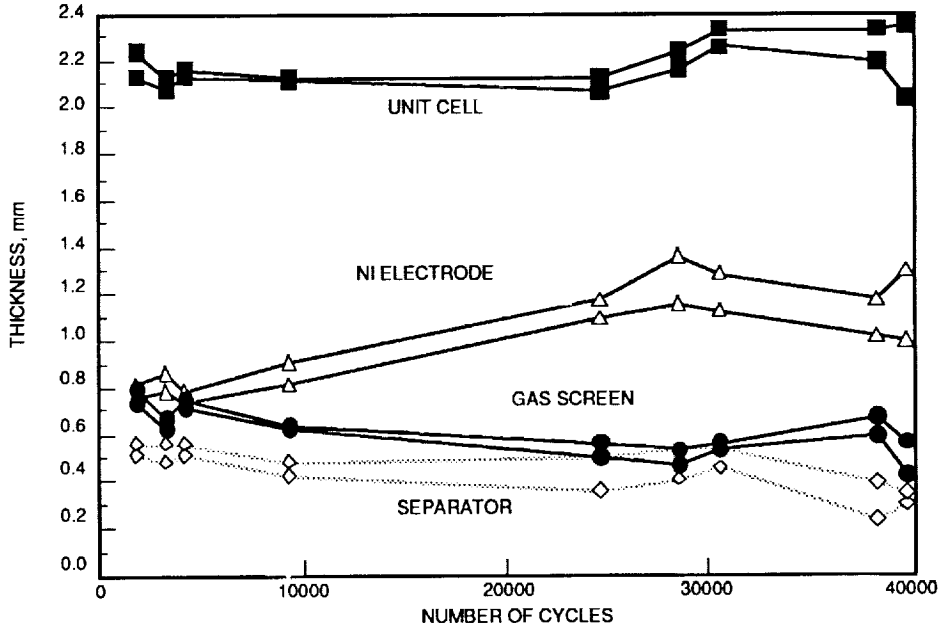

FIGURE 9. PLOTS OF CELL STACK COMPONENTS THICKNESS AS A FUNCTION OF CYCLING.

TABLE 4. FLOODED CAPACITIES OF NICKEL ELECTRODES FROM CYCLED CELLS. #1: TOP ELECTRODE OF THE STACK. #6 BOTTOM ELECTRODE OF THE STACK. A NEW ELECTRODE HAD 1.24 AH FOR AN AVERAGE VALUE.

CELL NO. %	KOH CONC.	CAPACITY OF #1 ELECTRODE, AH				CAPACITY OF #6 ELECTRODE, AH				CAPACITY RATIO
		1ST	2ND	3RD	AV.	1ST	2ND	3RD	AV.	#6 / #1
BP1	21	1.17	1.18		1.18	1.24	1.24		1.24	1.05
BP2	26	1.18	1.17		1.17	1.25	1.24		1.25	1.07
BP3	26	0.99	1.00	1.00	1.00	0.70	0.69	0.70	0.70	0.70
BP4	31	1.16	1.11	1.12	1.13	0.73	0.77	0.79	0.76	0.67
BP5	31	0.98	0.96	0.98	0.97	0.69	0.70	0.71	0.70	0.72
BP6	36	0.98	1.08	1.17	1.08	0.69	0.81	0.81	0.77	0.72
BP7	21	0.95	0.93	0.93	0.94	1.01	1.02	1.01	1.01	1.08
BP8	26	1.21	1.15		1.18	1.13	1.11		1.12	0.95
BP10	23.5	1.26	1.26		1.26	1.24	1.24		1.24	0.98
(AFTER CHANGING ELECTROLYTE)										
BP1	31	1.11	1.10		1.11	1.16	1.15		1.16	1.04
BP2	31	1.13	1.23		1.18	1.16	1.15		1.16	0.98
BP3	31	1.02	1.04	1.03	1.03	0.75	0.77	0.77	0.76	0.74
BP4	31	1.14	1.14	1.14	1.14	0.79	0.80	0.80	0.80	0.70
BP5	31	1.01	1.03	1.03	1.02	0.72	0.72	0.72	0.72	0.72
BP6	31	1.04	1.04	1.03	1.04	0.69	0.70	0.70	0.70	0.68
BP7	31	1.02	1.06	1.05	1.04	1.03	1.09	1.08	1.07	1.03
BP8	31	1.21	1.20		1.21	1.06	1.05		1.06	0.88
BP10	31	1.21	1.20		1.21	1.21	1.20		1.21	1.00

Electrode Capacity in a Flooded Cell - Capacities of two nickel electrodes from each failed cell were measured in a flooded cell at C/2 discharge rate after charging C/10 for 18 to 19 hours. One electrode was from the top of the cell stack (#1) and the other was from the bottom of the stack (#6). Two to three capacities were measured in an electrolyte of the same KOH concentration as the original test cell and then all electrolytes were changed with 31% KOH for additional three capacities. The results are summarized in Table 4. With and exception of BP3 which was an anomalous cell, the capacity loss of nickel electrodes in low KOH concentration (21 to 26%) cells was relatively low and independent of the electrode position (#1 or #6) despite long cycling. With higher KOH concentrations (31 to 36%), however, the capacity of bottom (#6) nickel electrode was roughly 30% smaller than top (#1) electrode of the same cell. It appears that the cause of this faster degradation of the electrodes from the bottom (#6) than those from the top (#1) of the stack was originated from the variation of the electrolyte content from the top to the bottom. Cell teardown showed that the bottom part (#6) of the stack had much more electrolyte than the top part (#1) due to gravitational segregation. The wetter electrode pair (#6) is expected to pass higher current throughout the cycle test than the drier pair (#1) which was in parallel electrical connection. This uneven current distribution would have caused heavier usage of the #6 electrode than the #1. This heavy usage appears to cause a severe capacity decrease in higher KOH concentrations while the decrease is relatively minor in low KOH concentrations. No apparent relationship was found between the capacity decrease and the electrode expansion.

Chemical Analyses - Chemical Analyses results of electrolyte composition of cycled cells are shown in Table 5. The overall electrolyte concentrations in long cycled cells (BP2, BP8, and BP10) was increased by 3 to 4% from the initial value, indicating possible nickel plaque corrosion. Carbonate concentration which was negligible initially increased slightly in all cycled cells. The amount of carbonate build-up was roughly proportional to logarithmic number of cycles as shown in Figure 10. A possible source of carbonate might be corrosion of plaque which may contain about 0.1 % (by wt.) of carbon because it is made of carbonyl nickel powder (INCO Type 287).[6]

TABLE 5. COMPOSITION OF ELECTROLYTE FROM CYCLED CELLS.

CELL NO.	INITIAL CONC. OF KOH, %	KOH, % AS KOH	K_2CO_3, % AS KOH	TOTAL K^+ ION, % AS KOH	SAMPLING TECHNIQUE
BP2	26	25.5	5.27	30.77	SOXHLET*
BP3	26	23.6	2.7	26.3	BOTTOM OF CELL
BP4	31	28.0	3.3	31.3	BOTTOM OF CELL
BP6	36	33.2	2.5	35.7	BOTTOM OF CELL
BP7	21	17.3	4.0	21.3	BOTTOM OF CELL
BP8	26	24.03	5.07	29.1	SOXHLET*
BP10	23.5	21.6	5.1	26.7	SOXHLET*

* SOXHLET EXTRACTION OF #3 & 4 UNIT CELLS.

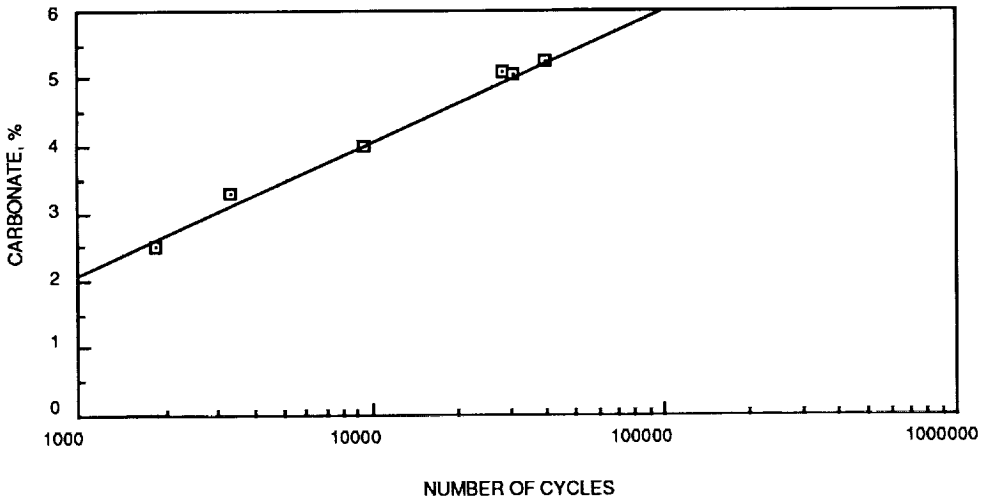

FIGURE 10. A PLOT OF CARBONATE BUILD-UP VS. NUMBER OF CYCLES.

TABLE 6. RESULTS OF CHEMICAL ANALYSES OF NEW AND CYCLED NICKEL ELECTRODES FROM BP CELLS. NUMERICAL VALUES IN THIS TABLE INDICATE AMOUNTS IN MMOLES/G OF ACTIVE MASS

	NEW 27-08	BP1	BP2	BP4	BP6	BP8	BP10
NI^{p} (SINTER)							
TITRATION (A)	8.29	4.92	3.70	7.79	8.41	4.99	4.59
AA	8.20	4.59	3.27	6.49	7.47	4.59	4.20
M (II&III); TITRATION.(B)	4.90	7.24	8.10	5.14	4.77	7.32	7.19
CO (II&III); AA	0.67	0.55	0.57	0.61	0.57	0.57	0.59
M (III)	1.50	0.90	1.78	0.58	0.80	2.60	1.40
TOTAL NI & CO TITRATION	13.40	12.06	11.94	12.20	12.56	12.23	11.87
(A) + (B)	13.19	12.16	11.80	12.93	13.18	12.31	11.78
(A) / [(A)+(B)], %	62.85	40.46	31.36	60.25	63.81	40.54	38.96

Chemical Analyses results of new and cycled nickel electrodes from test cells are shown in Table 6. Active material content (amount of total ionic Ni and Co in nickel electrode) is plotted against number of cycles in Figure 11. This content increased with cycling indicating that nickel plaque may be corroded gradually with cycling. Experimental data fit roughly to a linear corrosion rate of 0.1 Å/cycle (Curve A of Fig. 11).

In order to see if Pt was carried over the nickel electrode from adjacent H_2 electrode in BP cells in which soft shorts were developed. Elemental analyses (spectrographic) was carried out on outer edge of nickel electrodes from a few cycled cells. Analysis results of a nickel electrode from BP9 showed a considerable amount of Pt (0.25%) while Pt was not detected from a new electrode and detected only in trace level (less than 0.01%) in electrodes from BP2 and BP5. Considering both BP2 and BP9 had soft shorts, this non-uniform distribution of Pt might be due to a violent O_2 recombination ("popping") at peripheral edge as a probable mechanism of Pt migration.

Scanning Electron Microscope (SEM) - SEM pictures of a cross-sectional view of cell stack components were taken as a part of the failure analyses. Sample pictures of the components from cycled cells are shown in Figures 12, 13, and 14. BP6 (36%), which failed after relatively short cycling (1845 cycles), showed no apparent sign of expansion or deformation of stack components. However, long cycled cells, BP9 and BP2 (24,594 and 39,573 cycles, respectively) showed signs of heavy nickel electrode expansion, nickel active material migration, rupture of nickel sinter substrate, and deformation of other components such as separator, H_2 electrode, and gas screen material. It is interesting to note that despite the heavy expansion and sinter rupture in the long cycled electrodes, they suffered relatively small capacity decrease indicating that these changes are not direct causes of the electrode failure.

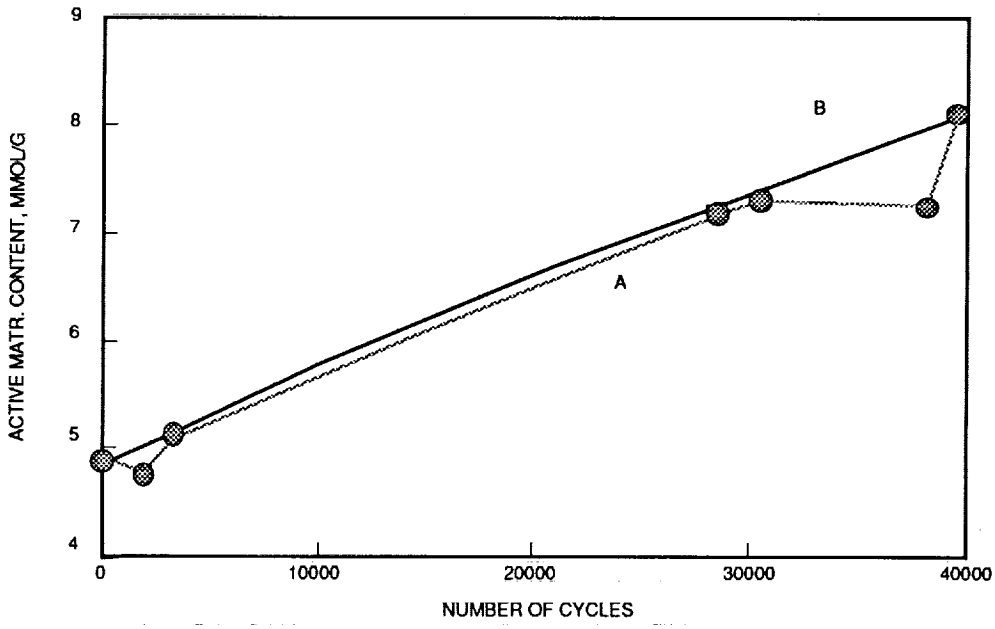

FIGURE 11. A PLOT OF ACTIVE MATERIAL CONTENT (TOTAL IONIC NICKEL AND COBALT) OF NICKEL ELECTRODE VS NUMBER OF CYCLES.

DISCUSSIONS

Cycle life of a nickel electrode increased greatly as the KOH concentration decreased in the electrolyte, although initial capacity of a nickel electrode decreases slightly as the concentration decreases reported earlier[1b]. The cycle life increased more than twice when the concentration was decreased from 36 to 31%. Although results with very low KOH concentration (21 to 23.5%) was complicated due to unusable low voltage secondary plateau formation[1c], the cycle life improved roughly nine times when the concentration was reduced to 26% from conventional value of 31%.

The failure mechanisms of a Ni/H_2 cell with a low KOH concentration (26% or lower) and one with a high KOH concentration (31% or higher) appears to be different from each other. High concentration cells failed on cycling by a gradual fading of nickel electrode capacity after relatively small number of cycles (1845 to 4230), while low concentration cells failed on cycling after a large number of cycles (mostly 25,000 to 40,000) by a "soft" short formation without an excessive capacity decrease of nickel electrodes. As a result of the tremendous difference in the number of cycles, heavy electrode expansion and active material migration and extrusion were observed in the long life low KOH concentration cells, but relatively small physical changes are present in the failed nickel electrodes in the high KOH concentration cells. However, we have observed much less "black powder" formation in BP7 (21% KOH) after 9402 cycles than in BP4 (31% KOH), BP5 (31% KOH), and BP6 (36% KOH) which were tested for less than half as many cycles as BP7, indicating that some physical changes occur at much reduced rate in low KOH concentrations.

The observation that no significant internal resistance change of cells despite heavy electrode expansion causing sinter rupture and active material migration and extrusion appears to indicate that the conductivity of nickel sinter may not be the controlling factor in electrode failure. We speculate that the capacity fading mechanism might involve crystallographic and micro morphological changes of active material. All long life cells failed eventually on cycling due to a "soft" short formation without an excessive capacity decrease of nickel electrodes as shown in Table 4. The positive identification of Pt on a nickel electrode (spectrographic analysis result) appear to indicate that the short might be due to the Pt on nickel electrode. This Pt might act as an hydrogen electrode while it is electrically shorted to the nickel electrode through a layer of high resistance nickel oxide/hydroxide material. An alternate mechanism might involve a short between nickel and hydrogen electrodes via extruded nickel active material in the gas screen area.

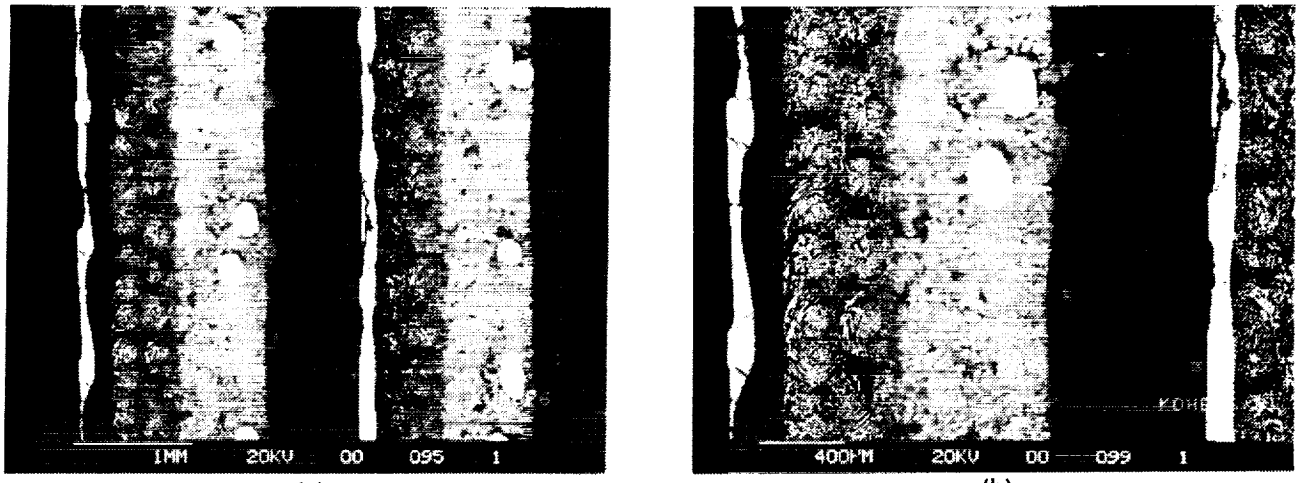

(a) (b)

FIGURE 12. SEM CROSS-SECTIONAL VIEW OF (A) #3 AND #4 CELLS AND (B) EXPANDED VIEW OF LOCAL AREA OF BP6.

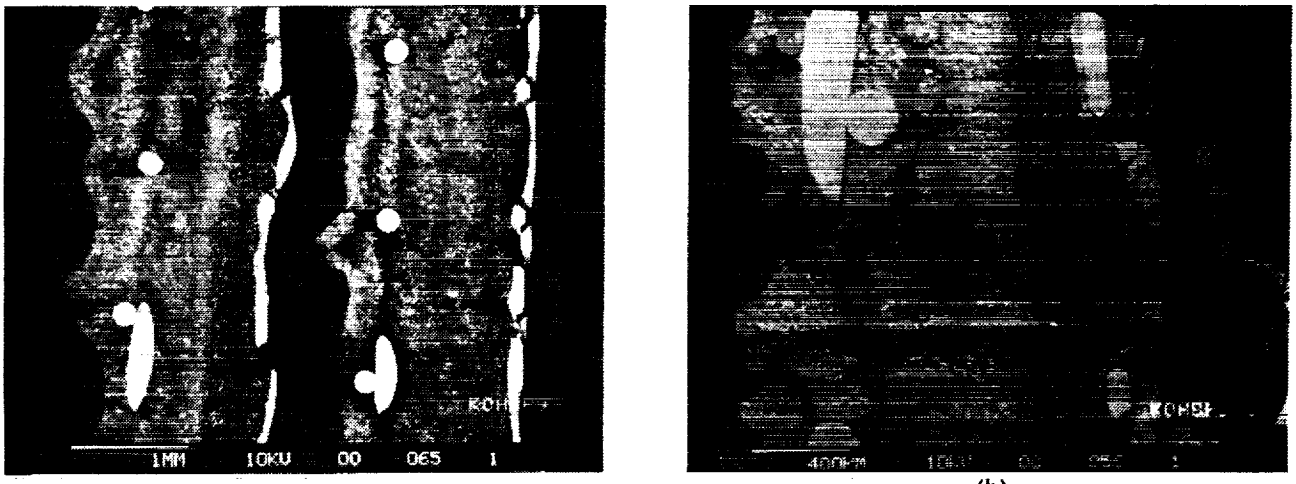

(a) (b)

FIGURE 13. SEM CROSS-SECTIONAL VIEW OF (A) #3 AND #4 CELLS AND (B) EXPANDED VIEW OF LOCAL AREA OF BP9.

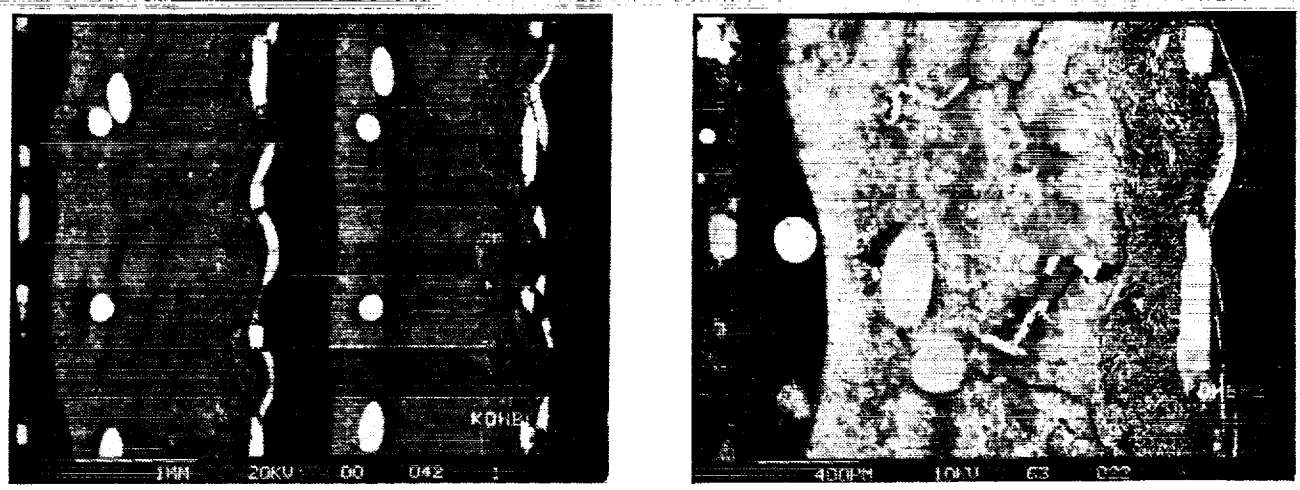

(a) (b)

FIGURE 14. SEM CROSS-SECTIONAL VIEW OF (A) #3 AND #4 CELLS AND (B) EXPANDED VIEW OF LOCAL AREA OF BP2.

ACKNOWLEDGMENT

We would like to acknowledge NASA-Lewis Research Center for its support for this study (Contract NAS 3-22238; Project Manager: John Smithrick).

REFERENCES

1. (a) H. S. Lim and S. A. Verzwyvelt, "KOH Concentration effect on the cycle life of nickel-hydrogen cells." Proc. 20th IECEC, August 1985, p. 1.165. (b) H. S. Lim and S. A. Verzwyvelt, " Cycle life of nickel-hydrogen cells. II. Accelerated cycle life test, " Proc. 21st IECEC, August 1986, p. 1601. (c) H. S. Lim and S. A. Verzwyvelt, " KOH concentration effect on the cycle life of nickel-hydrogen cells. III. Cycle life test, " J. Power Sources, 22, 213 (1988).

2. (a) H.S. Lim, "Long life nickel electrodes for nickel-hydrogen cells", Final Report of Phase I, NAS 3-22238, NASA Cr-174815. December, 1984; (b) H.S. Lim and S. A Verzwyvelt, "Long life nickel electrodes for a nickel-hydrogen cell: I. Initial Performance, " Proc. 18th IECEC, August 1983, p. 1543; (c) H.S. Lim and S. A Verzwyvelt, " Long life nickel electrodes for a nickel-hydrogen cell: Cycle life test," Proc. 31st Power Sources symposium, June 1984, Cherry Hill, NJ. p. 157; (d) H.S. Lim and S. A Verzwyvelt "Long life nickel electrodes for a nickel-hydrogen cell: Results of an accelerated test and failure analyses. " Proc. 19th IECEC, August 1984, p. 312

3. H. S. Lim and S. A. Verzwyvelt, ' Nickel electrode expansion and the effect of LiOH additive." Proc. 20th IECEC, August 1985, p. 1.104.

4. M. P. Bernhardt and D. W. Mauer, Proc. 29th Power Sources Conf. 1980, Electrochemical Society, p. 219.

5. P.P. McDermott, " Analysis of Nickel Electrode Behavior in an Accelerated Test." Proceedings of Symposium on the Nickel Electrode, Proc. Vol. 82-4, R. G. Gunther and S. Gross Eds. (The Electrochemical Society, Pennington, NJ, 1982), p. 224.

6 V. A. Tracy, "The properties and some applictions of carbonyl-nickel powdwers," Powder Metallurgy, 9, 54 (1966).